Optics Communications xxx (xxxx) xxx

Contents lists available at ScienceDirect

Optics Communications

journal homepage: www.elsevier.com/locate/optcom

Modelling domain switching of ferroelectric $BaTiO_3$ integrated in silicon photonic waveguides

M. Mishra [a], N.R. Das [a], A. Melloni [b], F. Morichetti [b,*]

[a] Institute of Radio Physics and Electronics, 92 A.P.C. Road, University of Calcutta, Kolkata 700009, WB, India
[b] Dipartimento di Elecctronica, Informazione e Bioingegneria, Politecnico di Milano, Via Ponzio 34/5, 20133, Milano, Italy

ARTICLE INFO

Keywords:
Integrated optics
Silicon photonics
Optical actuators
Ferroelectric materials

ABSTRACT

We present a model to investigate the local change of the refractive index of a ferroelectric material employed as upper cladding of silicon photonic waveguides. The model is used to predict the saturation voltage required to achieve complete domain switching in case of a $BaTiO_3$ film and to evaluate the performance of non-volatile phase-actuators integrated in silicon waveguides. Results show that the refractive index change associated with the domain switching of the $BaTiO_3$ cladding enables the realization of compact phase actuators with a length of few tens of micron. The proposed model has a general validity and can be used to other ferroelectric materials as well as to other semiconductor or dielectric waveguides.

1. Introduction

The scale of integration allowed by silicon photonics is enabling the evolution of photonic integrated circuits towards more and more complex architectures, including reconfigurable on chip networks and programmable photonic processors [1,2]. When a large number of tunable photonic elements needs to be controlled, it is essential to have efficient actuators to steer and keep photonic integrated circuits to the desired working point.

An optical actuator is any device that can be used to manipulate either the amplitude or the phase of the light. Therefore, also high-speed modulators and memristors can be considered as actuators. To calibrate and control the functionality of a photonic integrated circuit, phase actuators (also referred to as phase shifters) are required, which can be used to modify on-demand the phase delay of the light by changing the refractive index of either the core or cladding material of the waveguide. Phase actuators in silicon waveguides are typically realized by exploiting thermo-optic effect [3–7] and carrier injection/depletion in doped waveguides [8–12]. However, these types of actuators are volatile and need continuous supply of electrical power. The continuous consumption of power not only makes the device less energy efficient, but also makes the photonic circuit less suitable for low energy applications, such as space and submarine application etc., where power consumption is a major concern. Furthermore, when many components are densely integrated, thermo-optic actuators additionally suffer from mutual thermal crosstalk, which can impair the effectiveness.

Recently, an increasing interest has been given to the integration of ferroelectric materials, such as barium titanate ($BaTiO_3$), lead zirconate titanate (PZT) etc., in silicon waveguides [13–17]. In ferroelectric materials electro-optic effects (Pockels) can be exploited to realize fast phase modulation. However, the growth of $BaTiO_3$ films with a high crystalline degree on silicon waveguides poses challenging technological issues, since it requires the deposition of well controllable interlayer films to accommodate the lattice mismatch between $BaTiO_3$ and silicon.

A rather unexplored approach to realize integrated optical phase actuators is the exploitation of domain switching in ferroelectric materials. In ferroelectric material, with randomly oriented domains [18,19] of individual large electrical polarization, an electric field can be applied conveniently to switch the ferroelectric domains to get polarization in a particular direction. This process is much stable and non-volatile in nature [20–22], and has been successfully used as non-volatile memory elements from a long time [23–27].

Because of its hysteresis nature, polarization will be maintained even after the withdrawal of the field. Domain re-orientation leads to a change in the refractive index of the material. Since $BaTiO_3$ is a uniaxial material with a refractive index $n_o = 2.41$ along the ordinary axis and $n_e = 2.36$ along the extraordinary axis, domain orientation of ferroelectric $BaTiO_3$ from in plane (a-axis) to out of plane (c-axis) is expected to be associated to a large and non-volatile change of the local refractive index, on the order of about $\Delta n = n_o - n_e = 0.05$ [22]. We have recently observed a large ($\sim 10^{-2}$) non-volatile (>1 week) change of the refractive index of a film of polycrystalline $BaTiO_3$ which is associated with a 90° reorientation of the ferroelectric domains [28,29]. We have also demonstrated the possibility to integrate thin film of polycrystalline $BaTiO_3$ on silicon waveguides with a low additional propagation loss (<1 dB/mm) [28,29]. Preliminary results show that the switch of

* Corresponding author.
E-mail address: francesco.morichetti@polimi.it (F. Morichetti).

https://doi.org/10.1016/j.optcom.2019.05.001
Received 11 January 2019; Received in revised form 19 April 2019; Accepted 1 May 2019
Available online xxxx

Please cite this article as: M. Mishra, N.R. Das, A. Melloni et al., Modelling domain switching of ferroelectric $BaTiO_3$ integrated in silicon photonic waveguides, Optics Communications (2019), https://doi.org/10.1016/j.optcom.2019.05.001.

the refractive index may take place on a time scale of few tens of μs. The required switching speed strongly depends on the specific application. For instance, for reconfiguration operation in programmable photonic integrated circuits, the benchmark is given by thermal actuators, which have a response time of several microsecond, but they are volatile, and in silicon photonics they consume up to 10 mW per π shift. For these applications a non-volatile phase actuator with 10 microsecond speed would be extremely useful indeed.

Other works have proposed the use of non-volatile domain switching in $BaTiO_3$ [30] and multiferroic $BiFeO_3$ [30,31] plasmonic waveguide modulators to realize dynamic signal switching in photonic integrated circuits. These works focus on the optimization of the design of these devices, assuming a complete switching of the refractive index of the ferroelectric material (from ordinary to extraordinary index) across the whole structure. However, domain switching is expected to change locally because of the actual electric field configuration between the electrodes.

Though several models exist in literature for modelling domain switching in $BaTiO_3$ [32–38], these have never been applied to the case of $BaTiO_3$ films integrated in a silicon waveguide. Here, we describe a simple numerical model that can be used to predict the domain switching effect occurring in a silicon waveguide coated with a $BaTiO_3$ film on application of a voltage field, taking into consideration the local switch induced by the local electric field across the structure. Our model is general and can be applied to different waveguide geometry and to different ferroelectric materials. In Section 2, we introduce the waveguide structure considered in this work, consisting of a silicon channel waveguide covered with a $BaTiO_3$ upper cladding. In Section 3, we describe the proposed model, which is validated in Section 4 by comparing the results achieved on a case-study planar structure with numerical results reported in the literature. In Section 5 we apply our model to study the switching of the ferroelectric domains in the waveguide structure described in Section 2 and to predict the change of the optical properties on the waveguide induced by domain switching. Section 6 summarizes the main results of this work.

2. Device structure

The waveguide structure considered in this work is schematically depicted in Fig. 1. A Si channel waveguide is realized on a SiO_2 substrate and is covered with $BaTiO_3$ cladding. The width and height of the core is 500 nm and 300 nm respectively and the thickness of the $BaTiO_3$ cladding is 300 nm. On top of the $BaTiO_3$ cladding a 700 nm wide electrode is deposited, while other two electrodes are deposited on the same SiO_2 substrate at a distance of 200 nm, on both sides of the Si core, before the deposition of the $BaTiO_3$ cladding. As shown in the following of this paper, the distance between the electrodes should kept as small as possible in order to minimize the applied voltage. In order to avoid optical loss of the guided mode, transparent conductive oxides, such as indium tin oxide (ITO), could be conveniently employed. In the considered coordinate system, the propagation of light is along x direction, while y and z identify the horizontal (width) and the vertical (height) dimensions of the waveguide cross-section. Assuming the top electrode as the positive and the bottom electrodes as the ground electrodes, the electric field is applied in the $-z$ direction.

When an electric field greater than coercive field (E_c) is applied locally, the $BaTiO_3$ domains tend to change their dielectric polarization in order to align to the applied field. The resulting change of the $BaTiO_3$ refractive index leads to a net change of propagation constant of the light in the waveguide, and hence to a phase shift of the waveguide.

Electromagnetic simulations in Fig. 2(a) shows the computed TE and TM fundamental modes of the waveguide. By evaluating the mode overlap factor with the $BaTiO_3$ film, we see that overlap factor is larger for TM polarization reaching more than 25% when for a $BaTiO_3$ thickness t > 300 nm, while for TE polarization is about 17%. Assuming that the refractive index of the $BaTiO_3$ cladding can be modified up

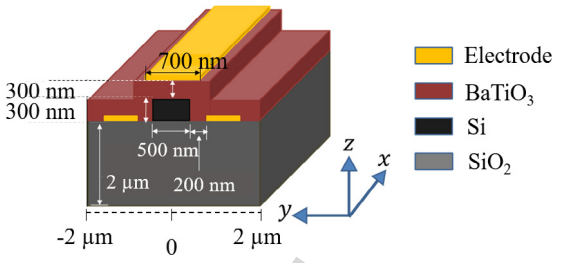

Fig. 1. Schematic of the silicon photonic waveguide actuator with ferroelectric ($BaTiO_3$) cladding.

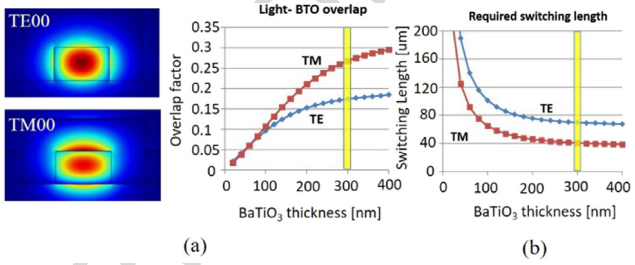

Fig. 2. (a) TE and TM fundamental modes of the Si waveguide and light $BaTiO_3$ overlap factor and (b) switching length of $BaTiO_3$ required for a π phase modulation in the propagating wave.

to $\Delta n = 0.05$ through an external electrical field, we evaluated the switching length as the minimum length of the waveguide actuator required to introduce a π-phase shift. Fig. 2(b) shows the plot for the switching length versus the thickness of the $BaTiO_3$ layer. When the thickness of the $BaTiO_3$ film is higher than 300 nm, a π-shift is expected to occur after a length of about 70 μm for TE polarization and 40 μm for TM polarization. Our simulations show that in this condition (t > 300 nm), the excess loss induced by a top ITO electrode, with an extinction coefficient of 0.1 at a wavelength of 1550 nm, is less than 10^{-3} dB/μm for TE polarization and about 2×10^{-3} dB/μm for TM polarization. Considering the switching length of Fig. 2(b), this results in an excess loss for the ferroelectric actuator of less than 0.1. It may be mentioned here that ITO can change its optical properties due to carrier accumulation at the surface when a voltage is applied. However, the overlap of the optical field with the ITO layer is extremely small (<5%) when the thickness of the BTO layer is 300 nm, which has been chosen as a trade-off between the switching length, the applied voltage and the excess loss induced by the ITO layer. Furthermore, when the voltage signal is switched off, the refractive index change in the $BaTiO_3$ layer is maintained (non-volatile effect), while the change of the optical properties due to the carrier accumulation layer at the ITO surface disappears (volatile effect). Therefore, the change in optical property of ITO will have no significant effect on the non-volatile switching behaviour of the device.

Because of the small overlap of the optical mode with the ITO electrodes, the change of the optical properties of the ITO material when a voltage signal is applied (for instance due to carrier accumulation at the surface, which is also a volatile effect) will have no relevant impact on the non-volatile switching behaviour of the device.

These results suggest the possibility to realize compact non-volatile phase actuators, with a length comparable to that of conventional volatile thermal actuators.

3. Numerical model

In this section, we present the numerical model developed to study the change of the refractive index profile of the ferroelectric $BaTiO_3$ cladding of a silicon waveguide upon the domain switching induced by

Please cite this article as: M. Mishra, N.R. Das, A. Melloni et al., Modelling domain switching of ferroelectric $BaTiO_3$ integrated in silicon photonic waveguides, Optics Communications (2019), https://doi.org/10.1016/j.optcom.2019.05.001.

an applied electric field. In our model we take into account that the coercive field E_c of $BaTiO_3$ strongly depends on its thickness (t) and increases for thinner layers because of the higher strain between the substrate and the $BaTiO_3$ layer increases [39–42]. To find the thickness dependence of E_c, we use the following relation derived from the normalized plot given in Ref. [42]

$$\frac{E_c}{E_{cR}} = (t \times 10^{6.5})^k \tag{1a}$$

where

$$k = m \log_{10} E_{cR}. \tag{1b}$$

E_{cR} is the value of E_c at $t = 10^{-6.5}$ m and is obtained as 5.09×10^6 V/m by using the value of E_c for $BaTiO_3$ at $t = 108$ nm taken from literature [43], and $m = -0.79$. Further, during the switching of domains, the value of E_c for the neighbouring un-polarized region slightly reduces due to strain between domains [44]. This fact has also been included in the present model.

To study the switching of orientation of a particular domain, we need to evaluate the local distribution of the applied electric field in the waveguide cross-section, which depends on the overall waveguide geometry and on the position of the electrodes. To this aim we carried out finite element method (FEM) simulations to obtain the vector electric field profile within the structure. Due to its hysteresis property, a ferroelectric material can be characterized by permanent electric polarization vectors, switching their orientation under the application of appropriate electric field. At equilibrium, two states of polarizations exist, namely positive polarization state (P_p) and negative polarization state (P_n). Under the influence of an applied electric field, interchange between P_p and P_n occurs depending upon the magnitude and orientation of the electric field components. If a positive electric field (E_p) greater than the positive coercive field (E_{cp}) is applied, then a differently orientated domain P_n changes its orientation in the direction of the field thus moving to a net positive state of polarization P_p in the ferroelectric material. Similarly the orientation can be changed by applying a negative electric field E_n greater (in magnitude) than the negative coercive field E_{cn}. It may be noted that the switching process of domains occur locally at each point of the material depending upon the magnitude and orientation (y or z-direction) of the local electric field components at that point. Now we see how the polarization state changes with electric field for its any particular orientation (y or z).

The net change in polarization state, on application of $E_p \geq E_{cp}$ is given by [45]

$$\Delta P_p = \left(1 - P_p\right)(f_p \Delta E), \tag{2}$$

where ΔP_p and ΔE are the incremental positive polarization state and incremental electric field respectively. The term $f_p \Delta E$ is the transition probability of domains from negative to positive polarization state, f_p being given by

$$f_p = \frac{1}{1 + e^{\frac{-(E_{lp} - E_{cp})}{E_o}}} \frac{1}{E_o}, \tag{3}$$

where E_{lp} is the local positive field and

$$E_o = \frac{KT}{q} \frac{1}{t}, \tag{4}$$

represents the field corresponding to the thermal voltage of the ferroelectric material. In Eq. (4), K is the Boltzmann's constant, T is temperature, q is electronic charge and t is thickness of the material ($BaTiO_3$).

From Eqs. (2) and (3) the following expression for P_p is derived

$$P_p = 1 - (1 - P_{ip}) \frac{1 + e^{\frac{-E_{ip} - E_{cp}}{E_o}}}{1 + e^{\frac{E_{lp} - E_{cp}}{E_o}}}, \tag{5}$$

where P_{ip} and E_{ip} are initial positive polarization state and initial positive field value respectively and E_{lp} represents the applied local positive field. Likewise, a similar expression for P_n is obtained

$$P_n = 1 - (1 - P_{in}) \frac{1 + e^{\frac{E_{in} + E_{cn}}{E_o}}}{1 + e^{\frac{-E_{ln} + E_{cn}}{E_o}}}, \tag{6}$$

where P_{in} and E_{in} are initial negative polarization state and initial negative field value respectively and E_{ln} represents the applied local negative field. The displacement vectors for positive and negative polarizations are obtained as [45]

$$D_p = P_s(2P_p - 1) \tag{7}$$

$$D_n = -P_s(2P_n - 1) \tag{8}$$

where P_s is the saturation polarization of the ferroelectric material under applied electric field. Using Eqs. (7) and (8) the hysteresis behaviour of $BaTiO_3$ can be obtained as a function of applied electric field, using the known parameters of the material. Fig. 3 shows hysteresis plot for three different thickness of $BaTiO_3$ layers, with coercive field scaling according to Eq. (1). In this case, we assume that the initial polarization is either saturated at positive (P_s) or negative ($-P_s$) polarization and we show the expected switch of the polarization state predicted by the proposed model when the thickness, and hence the coercive field, changes. It should be noted that the sharpness of the hysteresis curve, which strongly depends on the specific material, can be taken into account by adapting the transition probability function (3). Without loss of generality in the examples reported in this work we consider a nearly "ideal" ferroelectric materials with a sharp and a large hysteresis curve, but the proposed approach holds also in case of materials with a softer hysteresis curve.

The net local polarization across the $BaTiO_3$ film can be evaluated by including the effect of both y (P_y) and z-components (P_z) of polarization. As the polarization of domains in $BaTiO_3$ may grow more prominently in the longitudinal direction than in the lateral direction [20], in the model, we have added the possibility to include a higher weightage to P_z than to P_y (see Discussion). Besides, since the polarization change is in steps of 90°, i.e. it will have 0° or 90° orientation to maintain the minimum energy configuration of the material [46], in our model we convert the polarization into two states (either 0° or 90° orientation). Due to this, the local refractive index is binary and according to the domain orientation its value can be assigned as $n_0 = 2.41$ (ordinary axis) or $n_e = 2.36$ (extra ordinary axis) respectively [22]. For the non-polarized region of $BaTiO_3$, an intermediate refractive index value of 2.38 was assumed, thus, finally obtaining the local distribution of refractive index in the ferroelectric $BaTiO_3$ cladding, as a function of the applied electric field.

4. Model assessment

To assess the effectiveness of the model, we applied it to planar structures studied in the literature [46], namely the parallel plate capacitor of Fig. 4(a) and the structure of Fig. 4(b) to be used for piezoresponse force microscopy (PFM). In both cases, we assumed the same thickness $t = 64$ nm for the $BaTiO_3$ film, corresponding to a coercive field $E_c = 118$ kV/cm, and the same width of 32 nm of top electrode. The net spontaneous polarization of the native $BaTiO_3$ is considered to be zero.

Results in Fig. 5 show the polarization switching predicted by our model for different applied voltages. It can be observed that, for the capacitor model (a), the domain switching nucleation starts from both the electrodes, whereas in the PFM (b) it starts from the top electrode only. However, as the voltage increases, both cases evolves towards a polarization shape that is almost similar, except that the lateral spreading is little wider in the PFM structure as compared to the capacitor structure. When an electric field above E_c is applied, results nicely agree with those achieved by applying the phase field model on

Please cite this article as: M. Mishra, N.R. Das, A. Melloni et al., Modelling domain switching of ferroelectric $BaTiO_3$ integrated in silicon photonic waveguides, Optics Communications (2019), https://doi.org/10.1016/j.optcom.2019.05.001.

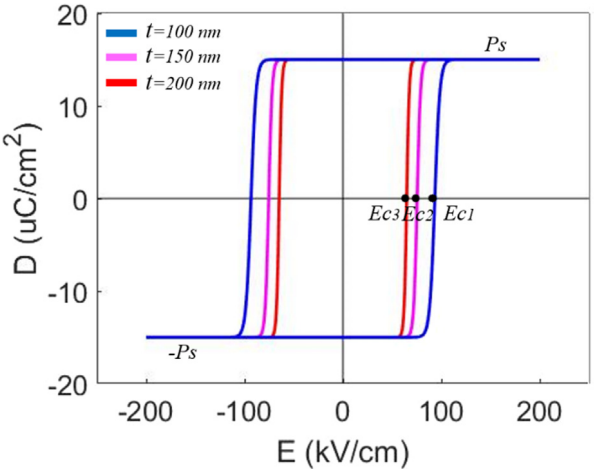

Fig. 3. The hysteresis curve obtained from the model for different thickness (t) of the $BaTiO_3$ at T = 298 K, assuming zero initial values for the electric field and saturated positive (P_s) or negative ($-P_s$) polarization state. The saturation polarization (P_s) is taken as 16 μC/cm^2 [47,48].

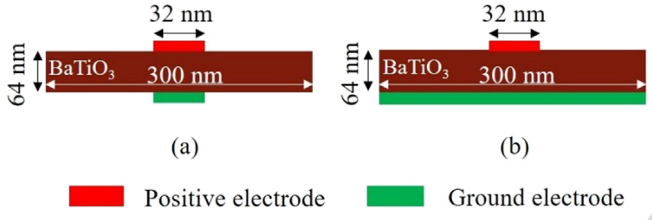

Fig. 4. Schematic of (a) capacitor and (b) PFM structure.

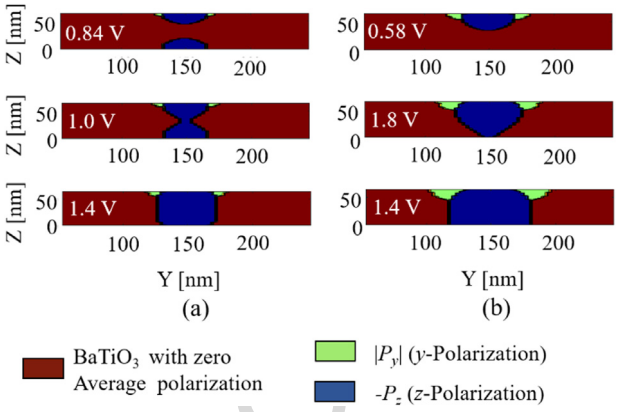

Fig. 5. Polarization switching in a planar $BaTiO_3$ film for t = 64 nm and E_c = 118 kV/cm for increasing applied voltage for (a) capacitor and (b) PFM structure.

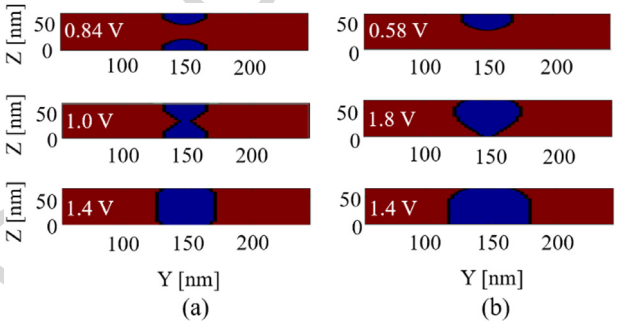

Fig. 6. Polarization switching in a planar $BaTiO_3$ film (t = 64 nm, E_c = 118 kV/cm) for increasing applied voltage when the P_y transition probability is scaled by 40% with respect to P_z transition probability: (a) capacitor and (b) PFM structure.

the same structure [46], the main difference being the appearance of a pronounced P_y region in the PFM structure at the sides of the top electrode.

This issue is solved by taking into account that, given the same local field, P_z and P_y domain switching may occur with a different transition probability, as explained in Section 3. In other words, when a local electric field is applied, the ferroelectric domains either switch to P_y or P_z, the most probable direction being strongly dependent on the material growth conditions [20]. Fig. 6 shows the result for the same capacitor and PFM structure, when the P_y transition probability is scaled by 40% with respect to P_z transition probability. With this assumption, by applying the same voltage values as in Fig. 5, only P_z polarization took place, with no occurrence of switching to P_y, this leading to a better agreement with results reported in [46].

When a polycrystalline film is considered, ferroelectric domains are natively randomly oriented. The actual domain orientation is strongly dependent of the deposition process. Crystallographic measurements (X-ray diffraction) performed on polycrystalline films show indeed the coexistence of in-plane and out-of-plane structural domains [29]. This means that there are domains that are mainly oriented in the plane of the film (a-axis) and other domains with out-of-plane orientation (c-axis). In our model we do not consider the existence of intermediate states, with domain orientation along arbitrary directions, but we assume that the material structure is the composition of in-plane and out-of plane domains.

5. Results

After the validation on a planar structure, we use the proposed model to study the polarization switching problem in the waveguide structure shown in Fig. 1. Fig. 7 shows local electric field components E_y (a) and E_z (b) across the waveguide, when a voltage of 14 V is applied between the top and the side electrodes. The electric field is normalized to the coercive field, which for a $BaTiO_3$ thickness of 300 nm is E_c = 52.3 kV/cm as indicated in the hysteresis plot of Fig. 7(d). Fig. 7(c) shows the electric field lines for V = 1 V. The permittivity of the $BaTiO_3$ film is assumed to be {1977, 1977, 112}.

Due to the electrode configuration, the field strength along z-axis is larger than that along y-axis in the $BaTiO_3$ cladding, this leading to a prominent domain switch along the z-axis. The magnitude of the local electric field normalized to the coercive field is shown in Fig. 8(a), this suggesting that local domain orientation is expected to change significantly along the $BaTiO_3$ cladding.

By applying the relations (2)–(8) and using the local field distribution as shown in Fig. 8(a), we obtain the corresponding local polarization plot as shown in Fig. 8(b). From the figures we see that, z-polarization (P_z) occurs in region where z-component of electric field (E_z) is dominant. Similar conclusion can be made for P_y also. The corresponding local refractive index profile of the $BaTiO_3$ layer along the z-component (n_z) and along y-component (n_y) are shown in Fig. 9. Depending on the applied voltage, domain switching occurs in different portions of the $BaTiO_3$ film, leading to a different refractive index profile for both n_z and n_y. The corresponding modified refractive index results from the anisotropic property of the material. The blue and green coloured areas represent the regions where the refractive index is equal to n_e and n_o respectively, while the reddish area represents the native $BaTiO_3$ having zero net polarization (n = 2.38).

It can also be noticed that, as the applied voltage increases, the area in which refractive index change takes place increases gradually near the waveguide core, and hence introducing incremental phase change in the light travelling through the waveguide. After a certain applied voltage, domain switching occurs in almost all the $BaTiO_3$ surrounding

Please cite this article as: M. Mishra, N.R. Das, A. Melloni et al., Modelling domain switching of ferroelectric $BaTiO_3$ integrated in silicon photonic waveguides, Optics Communications (2019), https://doi.org/10.1016/j.optcom.2019.05.001.

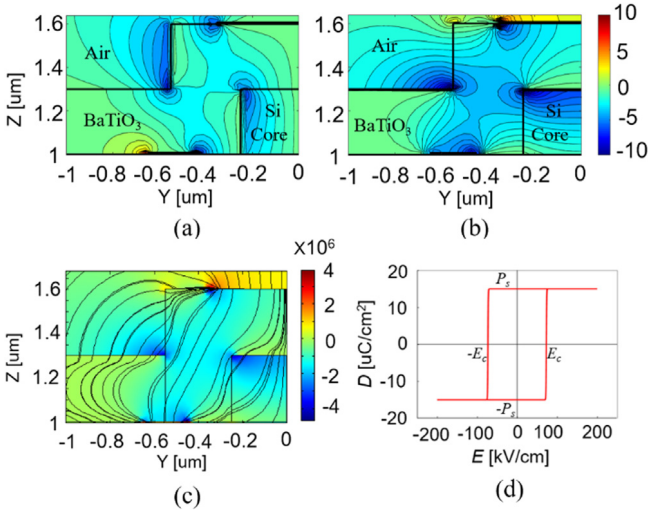

Fig. 7. Normalized local field components (a) E_y and (b) E_z, with respect to E_c (t = 300 nm) for 14 V. The black lines represent the outline of the waveguide structure and the position of the electrodes. Due to symmetry of the structure, only the left hand side of the structure is shown. (c) Electric field lines for V = 1 V. (d) Hysteresis plot for the 300 nm $BaTiO_3$ cladding layer.

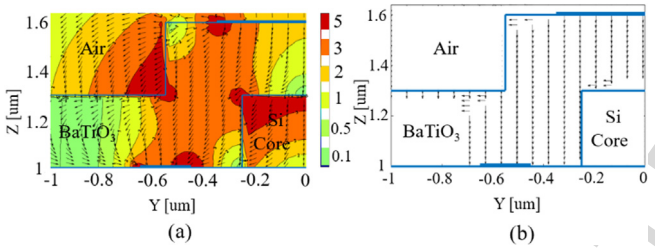

Fig. 8. (a) Amplitude (colour scale) and orientation (arrows) of the local electric field normalized to the coercive field of the $BaTiO_3$ cladding for an applied voltage of 14 V. (b) Expected local polarization across the $BaTiO_3$ cladding.

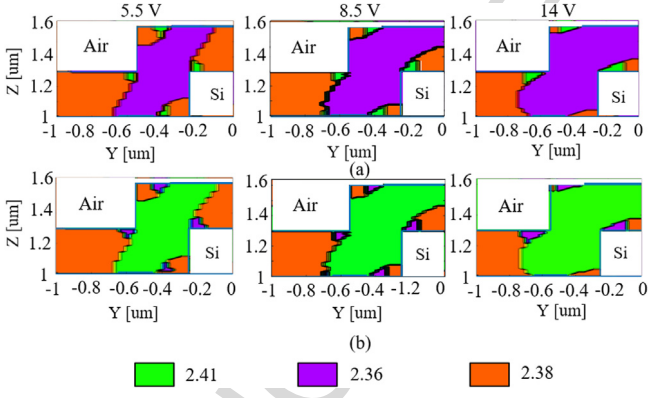

Fig. 9. Refractive index profile (a) n_z and (b) n_y of the $BaTiO_3$ cladding for an applied voltage 5.5 V, 8.5 V and 14 V respectively.

the waveguide core, leading to a refractive index change > 10^{-2} at saturation, as assumed in Section 1.

Fig. 10 shows the expected switching length for increasing applied voltage for TE and TM modes. To evaluate the switching length, electromagnetic simulations were carried out to calculate the effective index of the TE and TM modes of the waveguide with the modified refractive index profile in the $BaTiO_3$ cladding. These results are very well in line with the values reported in Fig. 2(b). It should be noted that, even though most of the cladding region gets switched at a voltage of about 8

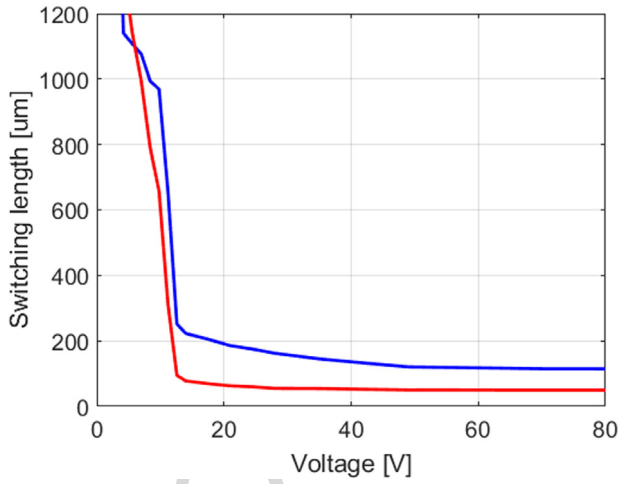

Fig. 10. Switching length of the $BaTiO_3$-coated waveguide of Fig. 1 as a function of the applied voltage for π-phase modulation of the TE (blue curve) and TM (red curve) guided modes. (For interpretation of the references to colour in this figure legend, the reader is referred to the web version of this article.)

V (see Fig. 9), at this voltage the switching length reported in Fig. 10 is as high as several hundreds of micron for both polarizations. The switching length steeply reduces when the voltage increases to nearly 13 V, because at this voltage the switch occurs also in the cladding regions adjacent to the Si core, where most of the evanescent field is concentrated (see Fig. 2). Thus, even though the corners of the device get a little sneered in practice, it will not have any noticeable change in the device performance. Therefore the switching length can be reduced by optimizing the design of the waveguide, for instance by narrowing the waveguide by increasing the overlap of the guided modes with the $BaTiO_3$ film or by optimizing the position and geometry of the electrodes.

In the examples considered in this work, we assumed an unpoled initial condition where the net spontaneous polarization of the $BaTiO_3$ film is zero (ferroelectric domains randomly oriented). If the material was initially poled with the ferroelectric domains oriented along preferential directions, the switching threshold would be expected to change, but increasing the electric field well above the coercive field the saturated spontaneous polarization would be only slightly dependent on the initial poling condition. However, the total refractive index change, which depends on the initial refractive index profile, could be rather different.

It is worth to point out that, in the considered waveguide structure, once domain switch has occurred for a certain applied voltage, by reversing the sign of the voltage the polarization state will be flipped by 180°. This means that the native polarization state would not be recovered. A possible way to bring the material back (or close) to the pristine state is by heating the waveguide above the Curie temperature (120 °C) in order to randomize the ferroelectric domains. Indeed, in [28,29] we observed that the native state of a polycrystalline $BaTiO_3$ film can be restored by a thermal treatment. Alternatively, another approach is to employ the three electrode waveguide of Fig. 1 in a way that each electrode is independently driven in order to apply a controllable voltage among any electrode pair. In this way a 90° domain switch could be effectively induced clockwise and counterclockwise by an all electrical control.

6. Conclusion

We presented a simple model to study the local change in the refractive index profile of a ferroelectric $BaTiO_3$ cladding of silicon photonic waveguides. The model effectiveness is validated through a

Please cite this article as: M. Mishra, N.R. Das, A. Melloni et al., Modelling domain switching of ferroelectric $BaTiO_3$ integrated in silicon photonic waveguides, Optics Communications (2019), https://doi.org/10.1016/j.optcom.2019.05.001.

comparison with the phase field model applied to the same planar structure of $BaTiO_3$ with a thickness of 64 nm. Numerical results on 300 nm $BaTiO_3$-coated silicon channel waveguide show the evolution of the local refractive index profile associated to domain switching across the waveguide cross-section. The model can be effectively used to predict the saturation voltage required to achieve complete domain switching in the ferroelectric film surrounding the waveguide core. Results show that the propagation constant of the guided modes is sufficiently large to enable the realization of phase actuators with a length of around 120 μm, which require less than 15 V driving voltage to provide a π-shift. Further optimization of the waveguide cross-section and of the electrode configuration is expected to reduce the footprint and the required voltage. However, it should be noted that the device performance, such as the energy consumption required for the switching, strongly depend also on the fabrication technology, and in particular on the quality of the ferroelectric material, which could indeed suffer from leakage current that increases power dissipation.

The model can be effectively used to optimize the waveguide geometry in order to maximize the mode overlap with the region where domain switching is more effective. Finally, it has a general validity and can be used to other ferroelectric materials as well as to other semiconductor or dielectric waveguides.

Acknowledgements

This work was supported by Erasmus Mundus LEADERS program, INSPIRE Fellowship program by Department of Science and Technology (DST) India [IF150280], and by Italian Fondazione Cariplo Project ACTIO [Rif. 2016-0881].

References

[1] Y. Shen, N.C. Harris, S. Skirlo, M. Prabhu, T. Baehr-Jones, M. Hochberg, X. Sun, S. Zhao, H. Larochelle, D. Englund, M. Soljafçifá, Deep learning with coherent nanophotonic circuits, Nature Photonics 11 (2017) 441.

[2] D. Pérez, I. Gasulla, L. Crudgington, D.J. Thomson, A.Z. Khokhar, K. Li, W. Cao, G.Z. Mashanovich, J. Capmany, Multipurpose silicon photonics signal processor core, Nature Commun. 8 (2017) 636.

[3] M.W. Pruessner, T.H. Stievater, M.S. Ferraro, W. S, Rabinovich thermo-optic tuning and switching in SOI waveguide Fabry–Perot microcavities, Opt. Express 15 (2007) 7557.

[4] J. Song, Q. Fang, S.H. Tao, T.Y. Liow, M.B. Yu, G.Q. Lo, D.L. Kwong, Fast and low power michelson interferometer thermo-optical switch on SOI, Opt. Soc. Amer. 15 (2008) 15304.

[5] I. Kiyat, A. Aydinli, N. Dagli, Low-power thermooptical tuning of SOI resonator switch, IEEE Photonics Technol. Lett. 18 (2006) 364.

[6] A. Densmore, S. Janz, R. Ma, J.H. Schmid, D.-X. Xu, A. Delâge, J. Lapointe, M. Vachon, P. Cheben, Compact and low power thermo-optic switch using folded silicon waveguides, Opt. Soc. Amer. 17 (2009) 10457.

[7] Y. Li, J. Yu, S, Chen rearrangeable nonblocking SOI waveguide thermooptic 4×4 switch matrix with low insertion loss and fast response, IEEE Photonics Technol. Lett. 17 (2005) 1641.

[8] Q. Xu, S. Manipatruni, B. Schmidt, J. Shakya, M. Lipson, 12.5 Gbit/s carrier-injection-based silicon microring silicon modulators, Opt. Express 15 (2007) 430.

[9] C. Li, L. Zhou, A.W. Poon, Silicon microring carrier-injection-based modulators/switches with tunable extinction ratios and OR-logic switching by using waveguide cross-coupling, Opt. Express 15 (2007) 5069.

[10] J.-B. You, M. Park, J.-W. Park, G. Kim, 12.5 gbps optical modulation of silicon racetrack resonator based on carrier-depletion in asymmetric p-n diode, Opt. Express 16 (2008) 18340.

[11] N.-N. Feng, S. Liao, D. Feng, P. Dong, D. Zheng, H. Liang, R. Shafiiha, G. Li, J.E. Cunningham, A.V. Krishnamoorthy, M. Asghari, High speed carrier-depletion modulators with 1.4v-cm vπl integrated on 0.25μm silicon-oninsulator waveguides, Opt. Express 18 (2010) 7994.

[12] Z.-Y. Li, D.-X. Xu, W.R. McKinnon, S. Janz, J.H. Schmid, P. Cheben, J.-Z. Yu, Silicon waveguide modulator based on carrier depletion in periodically interleaved PN junctions, Opt. Express 17 (2009) 15947.

[13] S. Abel, T. Stöferle, C. Marchiori, D. Caimi, L. Czornomaz, M. Stuckelberger, M. Sousa, B.J. Offrein, J. Fompeyrine, A hybrid barium titanate–silicon photonics platform for ultraefficient electro-optic tuning, J. Lightwave Technol. 34 (2016) 1688.

[14] S. Abel, T. Stöferle, C. Marchiori, D. Caimi, L. Czornomaz, C. Rossel, M.D. Rossell, R. Erni, M. Sousa, H. Siegwart, J. Hofrichter, M. Stuckelberger, A. Chelnokov, B.J. Offrein, J. Fompeyrine, Electro-Optical Active Barium Titanate Thin Films in Silicon Photonics Devices, Advanced Photonics Congress (OSA), 2013. (https://doi.org/10.1364/IPRSN.2013.IW4A.5).

[15] C. Xiong, W.H.P. Pernice, J.H. Ngai, J.W. Reiner, D. Kumah, F.J. Walker, C.H. Ahn, H.X. Tang, Active silicon integrated nanophotonics: ferroelectric batio3 devices, NANO Lett. 14 (2014) 1419.

[16] K. Alexander, John P. George, J. Verbist, K. Neyts, B. Kuyken, D. Thourhout, J. Beeckman, Nanophotonic pockels modulators on a silicon nitride platform, Nature Commun. 9 (2018) 3444.

[17] M. Hsu, A. Marinelli, C. Merckling, M. Pantouvaki, J. Campenhout, P. Absil, D.V. Thourhout, Orientation dependent electro-optical response of $BaTiO_3$ on $SrTiO_3$-buffered Si(001) studied via Spectroscopic Ellipsometry, Opt. Mater. Express. 7 (2017) 2030.

[18] S. Abel, T. Stoferle, C. Marchiori, C. Rossel, M.D. Rossell, R. Erni, D. Caimi, M. Sousa, A. Chelnokov, B.J. Offrein, J. Fompeyrine, A strong electro-optically active lead free ferroelectric integrated on slicon, Nature Commun. 4 (2013) 1671.

[19] P. Castera, A.M. Gutierrez, D. Tulli, S. Cueff, R. Orobtchouk, P.R. Romeo, G. Girons, P. Sanchis, Electro-optical modulation based on pockels effect in batiowithin a multi-domain structure, IEEE Photonics Tech. Lett. 28 (2016) 990.

[20] W.J. Merz, Domain formation and domain wall motions in ferroelectric $BaTiO_3$ single crystals, Phys. Rev. 95 (1954) 690.

[21] R.C. Miller, A. Savage, Motion of 180^0 domain walls in metal electroded barium titanate crystals as a function of electric field and sample thickness, J. Appl. Phys. 31 (1960) 662.

[22] M.J. Dicken, L.A. Sweatlock, D. Pacifici, H.J. Lezec, K. Bhattcharya, H.A. Atwater, Electrooptic modulation in thin film barium titanate plasmonic interferometers, Nano Lett. 8 (2008) 4048.

[23] D.E. Sawyer, D.B. Sandstrom, A semiconductor-ferroelectric memory device, IEEE Proc. 59 (1971) 87.

[24] I. Salaoru, S. Paul, Electrical bistability in a composite of polymer and barium titanate nanoparticles, Philoshopical Trans. A 367 (2009) 4237.

[25] U. Valiyaneerilakkal, S. Varghese, Poly (vinylidene fluoride-trifluoroethylene)/barium titanate nanocomposite for ferroelectric nonvolatile memory devices, AIP Adv. 3 (2013) 042131.

[26] S. Paul, D. Kumar, Manokamna, Gagandeep, Barium titanate as a ferroelectric and piezoelectric ceramics, J. Biosphere 2 (2013) 55.

[27] O. Auciello, J.F. Scott, R. Ramesh, THE PHYSICS OF Ferroelectric MEMORIES, Phys. Today 51 (1998) 22.

[28] M. Albo, S. Varotto, M. Asa, C. Rinaldi, M. Cantoni, R. Bertacco, F. Morichetti, Non-volatile switching of polycrystalline barium titanate films integrated in silicon photonic waveguides, in: Advanced Photonics 2018 (BGPP, IPR, NP, NOMA, Sensors, Networks, SPPCom, SOF), OSA Technical Digest (Online), Paper ITu4I.2, Optical Society of America, 2018.

[29] I.M. Albo, S. Varotto, M. Asa, C. Rinaldi, M. Cantoni, R. Bertacco, F. Morichetti, Integration of non-volatile ferroelectric actuators in silicon photonics circuits, in: 2018 20th International Conference on Transparent Optical Networks (ICTON), Bucharest, 2018, pp. 1–4.

[30] Viktoriia E. Babicheva, Andrei V. Lavrinenko, A plasmonic modulator based on a metal-insulator–metal waveguide with a barium titanate core, Photonics Lett. Poland 5 (2013) 57.

[31] Viktoriia E. Babicheva, Sergei V. Zhukovsky, Andrei V. Lavrinenko, Bismuth ferrite as low loss switchable material for plasmonic waveguide modulator, Opt. Express. 22 (2014) 28890.

[32] S. Choudhury, Y.L. Li, C.E. Krill III, L.-Q. Chen, Phase-field simulation of polarization switching and domain evolution in ferroelectric polycrystals, Acta Mater. 53 (2005) 5313.

[33] T. Koyama, H. Onodera, Phase-field simulation of ferroelectric domain microstructure changes in BaTiO3, Mater. Trans. 50 (2009) 970.

[34] S.C. Hwang, R.M. McMeeking, A finite element model of ferroelectric polycrystals, Ferroelectrics (OPA) 211 (1997) 177.

[35] A. Kumar, U.V. Waghmare, First-principles free energies and ginzburg-landau theory of domains and ferroelectric phase transitions in $BaTiO_3$, Phys. Rev. B 82 (2010) 054117.

[36] A. Kontsos, C.M. Landis, Phase-field modeling of domain structure energetics and evolution in ferroelectric thin films, J. Appl. Mech. 77 (2010) 041014.

[37] F.X. Li, R.K.N.D. Rajapakse, Nonlinear finite element modeling of polycrystalline ferroelectrics based on constrained domain switching, Comput. Mater. Sci. 44 (2008) 322.

[38] A.Y. Woldman, C.M. Landis, Phase-field modeling of ferroelectric to paraelectric phase boundary structures in single-crystal barium titanate, Smart Mater. Struct. 25 (2016) 035033.

[39] W.J. Mertz, Switching time in ferroelectric $BaTiO_3$ and its dependence on crystal thickness, J. Appl. Phys. 27 (1956) 938.

[40] N. Yanase, K. Abe, N. Fukushima, T. Kawakubo, Thickness dependence of ferroelectricity in heteroepitaxial $BaTiO_3$ thin film Capacitors, Japan. J. Appl. Phys. 38 (1999) 5305.

[41] G. Liu, C.-W. Nan, Thickness dependence of polarization in ferroelectric perovskite thin films, J. Phys. D: Appl. Phys. 38 (2005) 584.

Please cite this article as: M. Mishra, N.R. Das, A. Melloni et al., Modelling domain switching of ferroelectric $BaTiO_3$ integrated in silicon photonic waveguides, Optics Communications (2019), https://doi.org/10.1016/j.optcom.2019.05.001.

[42] K.M. Rabe, C.H. Ahn, J.-M. Triscone (Eds.), Phys. Ferroelectrics, Springer, 2007, p. 105.
[43] L. Huang, Z. Chen, J.D. Wilson, S. Banerjee, R.D. Robinson, I.P. Herman, R. Laibowitz, S. Obrien, Barium titanate nanocrystals and nanocrystal thinfilms: Synthesis, ferroelectricity, and dielectric properties, J. Appl. Opt. 100 (2006) 034316.
[44] H. Miyazawa, E. Natori, T. Shimoda, H. Kishimoto, F. Ishii, T. Oguchi, Relationship between lattice deformation and polarization in $BaTiO_3$, Japan. J. Appl. Phys. 40 (2001) 5809.
[45] K. Lim, K. Kim, S. Hong, K. Lee, A semi-empirical cad model of ferroelectric capacitor for circuit simulation, Integr. Ferroelectrics (OPA) 17 (1997) 97.
[46] N. Ng, R. Ahluwalia, H.B. Su, F. Boeyb, Lateral size and thickness dependence in ferroelectric nanostructures formed by localized domain switching, Acta Mater. 57 (2009) 2047.
[47] J.K. Hulm, Dielectric properties of single crystals of barium titanate, Nature 160 (1947) 127.
[48] A.F. Devonshire, I. Theory of Barium Titanate. Part, Theory of barium titanate, Part-I Phil. Mag. J. Sci. 40 (1949) 1040.

Please cite this article as: M. Mishra, N.R. Das, A. Melloni et al., Modelling domain switching of ferroelectric $BaTiO_3$ integrated in silicon photonic waveguides, Optics Communications (2019), https://doi.org/10.1016/j.optcom.2019.05.001.